BRILL

Nematology 28 (2026) 345-361

Nematology
brill.com/nemy

First integrative characterisation of the root-knot nematode, *Meloidogyne luci* infecting chickpea (*Cicer arietinum*) in Ethiopia

Habtamu KEFELEGN [1,2,3,4,*], Marjolein COUVREUR [1], Wim M.L. WESEMAEL [5,6], Beira H. MERESSA [2], André Machado BERTRAN [7], Jop WILTEN [7], Barbara GERIČ STARE [8], Nik SUSIČ [8], Nicole VIAENE [1,5], Misghina G. TEKLU [9] and Wim BERT [1,*]

[1] *Nematology Research Unit, Department of Biology, Ghent University, Ledeganckstraat 35, 9000 Ghent, Belgium*
[2] *College of Agriculture and Veterinary Medicine, Jimma University, P.O. Box 307, Jimma, Ethiopia*
[3] *College of Agriculture and Natural Resources, Debre Berhan University, PO. Box 445, Debre Berhan, Ethiopia*
[4] *Department of Zoology and Entomology, University of the Free State, PO Box 339, Bloemfontein 9300, South Africa*
[5] *Flanders Research Institute for Agriculture, Fisheries and Food (ILVO), Burg. Van Gansberghelaan 96, 9820 Merelbeke-Melle, Belgium*
[6] *Laboratory for Agrozoology, Department of Plants and Crops, Ghent University, Coupure links 653, 9000 Ghent, Belgium*
[7] *HLB BV, Kampsweg 27, 9418 PD Wijster, The Netherlands*
[8] *Plant Protection Department, Agricultural Institute of Slovenia, Hacquetova ulica 17, SI-1000 Ljubljana, Slovenia*
[9] *Plant Research, Plant Sciences Group, Wageningen University and Research Centre, PO. Box 16, 6700 AA Wageningen, The Netherlands*

ORCID iDs: Kefelegn: 0000-0003-2857-9483; Couvreur: 0009-0007-6831-4400; Wesemael: 0000-0001-7960-797X; Meressa: 0000-0001-9554-5393; Bertran: 0000-0002-8993-4357; Wilten: 0009-0000-6895-5610; Gerič Stare: 0000-0002-2334-8830; Susič: 0000-0002-6794-3703; Viaene: 0000-0002-7709-2578; Teklu: 0000-0002-1686-1089; Bert: 0000-0002-5864-412X

Received: 22 November 2025; revised: 3 February 2026
Accepted for publication: 27 February 2026; published online: 24 March 2026

Summary – A population of *Meloidogyne luci*, previously detected during a 2021 survey of nematodes associated with chickpea in Ethiopia, was maintained on tomato plants and characterised through morphological analysis, multiple molecular markers and complete mitogenome sequencing. Sequence comparison and phylogenetic analyses of the D2-D3 region of the 28S rDNA, ITS rDNA, and mtDNA (*Nad5*, *cox2* and *cox1*) revealed limited resolution in distinguishing *M. luci* from closely related species such as *M. ethiopica*, *M. inornata* and *M. hispanica*, underscoring the challenges of differentiating these taxa using partial gene sequences. Complete mitogenome sequencing yielded an 18 702 bp genome with 99.9% identity to the *M. luci* reference mitogenome. The genome comprised 11 open reading frames, 8 tRNAs, 2 rRNAs, and additional repeat regions, including extra genes such as *atp6* and *trnM*. A host status test confirmed the susceptibility of the chickpea cultivar 'Arerti' to *M. luci*, indicating that this highly polyphagous nematode poses a potential threat to chickpea production in Ethiopia.

Keywords – DNA barcoding, genomics, host status, mitogenome, molecular, morphology, phylogeny, root-knot nematodes, SEM, taxonomy.

Chickpea (*Cicer arietinum* L.) is the world's second most important food legume after common bean (*Phaseolus vulgaris* L.). It is cultivated across a wide range of climates, from tropical to temperate regions, with major production areas in South and West Asia, East and North Africa, Southern Europe, the Americas, and Australia (FAOSTAT, 2022).

Among the various constraints affecting chickpea production, plant-parasitic nematodes, particularly root-knot nematodes (*Meloidogyne* spp.) represent a significant but

* Corresponding authors, e-mails: habtamukefelegn@gmail.com; Wim.Bert@ugent.be

 | DOI: 10.1163/15685411-bja10472
 | ISSN: 1388-5545 (print) 1568-5411 (online)

often overlooked threat in Ethiopia (Kefelegn *et al*., 2024). This genus is considered the most destructive group in agriculture (Jones *et al*., 2013). To date, over 100 *Meloidogyne* species have been described, 22 of which are reported from Africa (Onkendi *et al*., 2014; Subbotin *et al*., 2021). In Ethiopia, six root-knot nematode species namely, *M. arenaria*, *M. incognita*, *M. javanica*, *M. ethiopica*, *M. hapla*, and other unidentified *Meloidogyne* sp. have been documented from various crops (Mandefro & Dagne, 2000; Meressa *et al*., 2014; Seid *et al*., 2019). Of these, *M. javanica*, *M. incognita*, *M. luci*, and an unidentified *Meloidogyne* sp. have been reported on chickpea roots (Sharma *et al*., 1992; Kefelegn *et al*., 2024, 2025).

Accurate identification of tropical root-knot nematodes remains difficult because of their recent species divergence and hybrid origins, which create considerable taxonomic ambiguity (Lunt *et al*., 2014; Janssen *et al*., 2016). For example, populations in Europe initially identified as *M. ethiopica* were later confirmed to be *M. luci* (Gerič Stare *et al*., 2017). *Meloidogyne ethiopica* was first reported in Tanzania by Whitehead (1968) and later confirmed in Ethiopia, Kenya, Mozambique, Zimbabwe and South Africa, as well as in Chile, Brazil and Peru (Carneiro *et al*., 2003). *Meloidogyne luci* was formally described in 2014 from isolates collected from lavender (*Lavandula spica* L.) in Brazil (Carneiro *et al*., 2014). Since then, it has been recorded on a wide range of crops, including cucumber (*Cucumis sativus* L.), lettuce (*Lactuca sativa* L.), broccoli (*Brassica oleracea* L. var. *italica*), okra (*Abelmoschus esculentus* (L.) Moench), green bean (*Phaseolus vulgaris* L.), yacon (*Polymnia sonchifolia* Poepp. Endl.) and kiwi (*Actinidia deliciosa* Planch.) in Brazil, grapevine (*Vitis vinifera* L.) and rose (*Rosa* sp. L.) in Chile, snapdragon (*Antirrhinum majus* L.) in Iran (Carneiro *et al*., 2014). It has also been reported to be associated with chickpea (*Cicer arietinum* L.) and tomato (*Solanum lycopersicum* L.) in Türkiye and Ethiopia (Şen & Aydinli, 2021; Kefelegn *et al*., 2025), common bean (*Phaseolus vulgaris* L.), pea (*Pisum sativum* L.) and soybean (*Glycine max* (L.) Merr.) in Brazil (Bellé *et al*., 2016), with tomato, the weed common groundsel (*Senecio vulgaris* L.) in Serbia and Slovenia (Gerič Stare *et al*., 2017; Susič *et al*., 2020a; Bačić *et al*., 2023), carrot (*Daucus carota*) and tomato in Iran and Guatemala (Janssen *et al*., 2016), and potato (*Solanum tuberosum* L.), ornamental plants and tomato in Portugal (Maleita *et al*., 2018; Santos *et al*., 2019; Rusinque *et al*., 2021). Moreover, a nematode population initially reported as *M. ethiopica* infecting maize (*Zea mays* L.) and kiwi in Greece (Conceição *et al*., 2012) was later re-identified as *M. luci* (Gerič Stare *et al*., 2017). Although no quantitative assessments of the economic impact of *M. ethiopica* and *M. luci* are available, both species remain serious threats to plant health and have been added to the EPPO alert list in 2023 (EPPO, 2023).

Recent studies have emphasised the need for integrative characterisation to ensure accurate identification of tropical *Meloidogyne* species, with *M. luci* being a prime example (Gerič Stare *et al*., 2017, 2019; Maleita *et al*., 2018). This study builds on the first confirmed report of *M. luci* in Africa, which relied on D2-D3 rDNA, *Nad5*, *cox1*, and *cox2* mtDNA sequences, *M. luci*-specific primers, and esterase isozyme profiles (Kefelegn *et al*., 2025). Here, an integrative approach was applied, combining morphological characterisation using light microscopy (LM) and scanning electron microscopy (SEM) with additional molecular analysis, including additional D2-D3 rDNA, *Nad5*, *cox1* and c*ox2* mtDNA sequences, as well as new ITS rDNA sequences. For LM and SEM, an improved spicule-isolation technique is described. In addition, a complete mitogenome assembly was generated to provide a comprehensive characterisation of the species.

Materials and methods

Nematode populations and pure cultures

During a 2021 survey conducted across Ethiopia's major chickpea growing areas, galled roots were collected from infected chickpea plants (Kefelegn *et al*., 2024). Populations of *M. luci* were obtained from galled roots of the chickpea 'Arerti' in the Minjar district, Ethiopia (8°54′21.1″N, 39°24′46.5″E) and identified as *M. luci* using *M. luci*-specific primers and esterase isozyme pattern analysis (Kefelegn *et al*., 2025). These populations were further studied after being established from single egg masses and subsequently maintained on the tomato '*Marmande*' under greenhouse conditions at the Flemish Research Institute for Agriculture, Fisheries and Food (ILVO) in Merelbeke-Melle, Belgium. These populations were used for morphological and molecular characterisations, including single barcodes and mitogenome using next-generation sequencing (NGS).

Morphological characterisation

Morphological and morphometric data were recorded from both temporary and permanent slides, following

Kefelegn *et al*. (2023). The nematodes mounted on these slides were measured and photographed using an Olympus BX51 DIC microscope (Olympus Optical, Tokyo, Japan), equipped with an HD Ultra camera. For scanning electron microscopy (SEM), nematodes were fixed in Trump's fixative, rinsed in 0.1 M phosphate buffer (pH 7.5), dehydrated through a graded series of ethanol solutions, critical point dried with liquid CO_2, and mounted on stubs using carbon tabs (double conductive tapes). They were subsequently coated with 25 nm of gold and imaged using a JSM-840 EM (JEOL) at 12 kV (Singh *et al*., 2021).

Improved spicules isolation techniques for LM and SEM

In the original method by Eisenback (1985), live male nematodes were transferred into a drop of 40% lactic acid for excision of spicules. The lactic acid was removed with a fine micropipette, followed by the addition of formalin without centrifugation. Formalin was absorbed with filter paper, and spicules were air-dried and marked using a glass rod for LM and SEM observation. Stylet dissection followed a similar procedure, replacing 45% lactic acid with 0.1% sodium hypochlorite (NaOCl) (Eisenback, 1985). This classical approach is well established and can be performed reliably by trained nematologists; however, it requires careful manual manipulation and precise pressure to avoid damaging delicate structures, particularly during stylet extraction (Mota & Eisenback, 1993).

To minimise manual manipulation, an alternative centrifugation-based approach for spicule isolation was developed. Tails from 25 *M. luci* males were transferred into a 200 μl tube containing 10 μl of distilled water. Then, 10 μl of 1% (NaOCl) solution (prepared from 3% household bleach) was added, and the mixture was sonicated for 3 min. The reaction was stopped by adding 50 μl of 4% formalin solution, followed by incubation at room temperature for 5 min. Spicules were then settled by centrifugation at 14 000 rpm for 5 min, after which approximately 30 μl of the supernatant was carefully removed by pipetting from the surface without disturbing the pellet. The spicules were then washed three times with distilled water, each time followed by centrifugation and removal of the supernatant. For LM, the pellet was resuspended in a final volume of 15 μl, and 10 μl of the suspension was placed in a small drop of glycerin on a microscope slide, over which a coverslip was carefully placed and examined under LM. For SEM, spicules were dehydrated through an ethanol series (50, 75, 95 and 100%). Each dehydration step involved the addition of ethanol, followed by centrifugation and careful removal of the supernatant. Once in 100% ethanol, the supernatant was carefully removed, and the spicules were left to air-dried overnight. The next day, the tube tip containing the dried spicules was cut and mounted onto an SEM stub, sputter-coated with gold, and imaged using SEM. The same protocol was also tested for stylet dissection but proved unsuitable, as the stylet knobs dissolved more rapidly than the surrounding head cuticle, compromising structural integrity during NaOCl treatment.

Single barcodes: DNA extraction, PCR amplification and sequencing

Genomic DNA was extracted from live second-stage juveniles (J2) and males. Briefly, individual nematodes were cut and transferred to a PCR tube containing 20 μl of worm lysis buffer (50 mM KCl, 10 mM Tris, pH 8.3, 2.5 mM $MgCl_2$, 0.45% NP-40 (Tergitol Sigma), and 0.45% Tween-20). The tubes were incubated at -20°C for 20 min, followed by the addition of 1 μl proteinase K (1.2 mg ml^{-1}). The mixture was then incubated at 65°C for 1 h, followed by 95°C for 10 min and then centrifuged at 14 000 rpm for 1 min (Singh *et al*., 2019). A 3 μl DNA template was added to a 23.5 μl master mix containing 10 μl of PCR water, 12.5 μl DreamTaq, and 0.5 μl of each primer (Kefelegn *et al*., 2023). PCR amplification was then performed using a Bio-Rad T100™ thermocycler. The primers, PCR conditions, and corresponding GenBank accession numbers for the D2-D3 region of 28S rDNA, ITS rDNA, and the mitochondrial genes *Cox1*, *Nad5* and *Cox2* are summarised in Table 1. After amplification, the PCR products were purified and sent to Macrogen (https://dna.macrogen.com) for DNA sequencing with the corresponding forward and reverse primers. The resulting sequence fragments (contigs) were assembled using Geneious Prime 2024, and the sequences were deposited in GenBank and assigned accession numbers (Table 1).

Mitochondrial genome: extraction, enrichment, amplification, sequencing and data analysis

Second-stage juveniles of *M. luci* were hatched in a mist chamber from infected tomato roots. Approximately 1800 J2 were collected in 40 ml of tap water in a 50 ml conical centrifuge tube and allowed to settle at room

Table 1. Primers and PCR conditions for the amplification of D2-D3 of 28S and ITS rDNA, as well as c*ox1*, *Nad5*, and *cox2* mtDNA genes, along with their respective GenBank accession numbers.

Target		Primer sequences ($5' \rightarrow 3'$)	References	Thermal profile	GenBank accession number
D2-D3 of 28S rDNA	D2A D3B	ACA AGT ACC GTG AGG GAA AGT TCGGAAGGAACCAGCTACTA	De Ley *et al*. (1999)	94°C 4 min; 40 × (94°C 1 min, 52°C 1 min 30 s, 72°C 2 min); 72°C 5 min	PQ454017*, PQ622663, PQ622664, PQ622665
ITS rDNA	Vrain2F Vrain2R	CTT TGT ACA CAC CGC CCG TCG TTT CAC TCG CCG TTA CTA AGG	Vrain *et al*. (1992)	94°C 4 min; 5 × (94°C 30 s, 64°C 30 s, 1°C per cycle ramp 3°C/s, 72°C 2 min); 30 × (94°C 30 s, 60°C 30 s, 72°C 1 min); 72°C 10 min	PQ610424, PQ610425, PQ610426, PQ610427
Cox1 mtDNA	JB3 JB4.5	TTT TTT GGG CAT CCT GAG GTT TAT TAA AGA AAG AAC ATA ATG AAA	Bowles *et al*. (1992); Derycke *et al*. (2010)	94°C 3 min; 42 × (94°C 30 s, 45°C 30 s, 72°C 1 min); 72°C 10 min	PQ448335*, PQ610476
Nad5 mtDNA	NAD5F2 NAD5R1	TAT TTT TTG TTT GAG ATA TAT CGTGAATCTTGATTTTCCATTTTT	Janssen *et al*. (2016)	94°C 2 min; 40 × (94°C 1 min, 45°C 1 min, 72°C 1 min 30 s); 72°C 10 min	PQ462657*, PQ619865
Cox2 mtDNA	COX2F COX2R	TTGAATTTAAGTGTTGTTTAT GATTAATACCACAAATCTCTG		94°C 2 min; 40 × (94°C 1 min, 45°C 30 s , 72°C 1 min); 72°C 10 min	OQ476238, OQ476239, OQ476240, PQ619863*
Species-specific	Mlf Mlr	ACTCCTGCGACCTCATGGCATTTA ACTCCTGCGAACACAACATTTACT	Maleita *et al*. (2021)	94°C 4 min; 35 × (94°C 30 s, 60°C 45 s, 72°C 45 s); 72°C	

Sequences marked with * were determined and published previously (Kefelegn *et al*., 2025).

temperature for 24 h. After removing the excess water, 1 ml (10%) Tween-20 was added, vortexed, and the suspension was transferred to 2 ml tubes (BIOplastics). Samples were centrifuged at 16 100 *g* for 2 min, and the pellets were combined to a final volume of approximately 75 μl. Genomic DNA was extracted using the NZYSoil gDNA isolation Kit (NZYTech) and eluted in 50 μl of elution buffer. DNA concentration was measured with a Qubit Fluorometer 3.0 (Thermo Scientific) using the dsDNA high sensitivity kit (Thermo Scientific). To enrich for circular mitochondrial DNA, 3.72 ng of total DNA was treated with Exonuclease V (NEB) in a 25 μl reaction containing 2.5 μl NEBuffer 4 (10×), 2.5 μl ATP, and 0.5 μl of the enzyme. The mixture was incubated at 37°C for 30 min, followed by EDTA addition (11 mM) and heat inactivation at 70°C for 30 min.

Two overlapping amplicons covering the complete mitochondrial genome were generated using proprietary primer sets (available upon request): CD534-CD536 (approx. 7.8 kb, amplicon 1) and CD559-CD560 (approx. 10 kb, amplicon 2). PCR reactions were performed in duplicate using LongAMP Master Mix (2X) (NEB) with 0.4 μM primers and 2 μl of enriched mtDNA in a 25 μl total volume. Duplicate PCR products were combined and purified with 1.8X AMPure XP beads (Beckman Coulter). The purified amplicons were eluted in 15 μl of nuclease-free water and quantified with Qubit Fluorometer 3.0 (Thermo Scientific). Sequencing libraries were prepared using the Native Barcod-

ing Kit (SQK-NBD114.24, Oxford Nanopore Technologies) following the ligation sequencing amplicon protocol (NBA_9168_v114_revQ_12Dec2024). Barcoded samples were pooled, ligated with native adapters, and approximately 50 fmol of library was loaded onto a MinION Mk1B device equipped with an R10.4.1 flow cell (FLO-MIN114). Sequencing was performed for 16 h using MinKNOW v24.11.10 with Dorado v7.6.8 for super-accurate base-calling and barcode trimming.

The resulting base-called reads were concatenated by barcode and quality-assessed using NanoPlot. Consensus sequences were generated using the Decona pipeline (Doorenspleet *et al*., 2025). Reads were filtered with NanoFilt (length: 7300-8000 bp for amplicon 1 and 10 200-11 200 bp for amplicon 2; $Q \geqslant 20$), clustered at 97% identity (minimum cluster size = 5) using CD-HIT and Minimap and polished sequentially with Racon and Medaka. Consensus sequences were mapped to the *M. luci* reference mtDNA (accession CACSLI010000066; project PRJEB27977) using CLC Main Workbench v25. Amplicons were merged to obtain the complete circular mtDNA, manually verified, and trimmed to remove adapter-derived sequences. Gene annotation was performed with MITOS2 (Donath *et al*., 2019), and tandem repeats were identified using the ETANDEM tool from the EMBOSS suite *via* the Galaxy platform (Rice *et al*., 2000; The Galaxy Community, 2024). Multiple sequence alignments (MSAs) were generated in Clustal Omega and curated manually in CLC Main Workbench v25. Phylogenetic relationships among *Meloidogyne* species were inferred using Maximum Likelihood analysis implemented in RAxML-ng (https://github.com/amkozlov/raxml-ng), and the resulting consensus trees were visualised in FigTree v1.4.4 (https://github.com/rambaut/figtree/releases).

Host status of chickpea cultivar to *M. luci*

In addition to assessing nematode density and reproduction factors (Kefelegn *et al*., 2025), plant height and total fresh root weight were recorded to further evaluate the impact of *M. luci* infection on chickpea growth. The chickpea 'Arerti' was used to assess host status and growth response to *M. luci*, under controlled temperature conditions in a growth chamber.

Results

Morphological characterisation

See Figs 1 and 2 and Table 2.

Juveniles

Body vermiform, 380-438 μm long; body annulated. Lateral field differentiation starts near the procorpus, forming two lines. Head region rounded, slightly set off from body. In SEM images, labial disc shows a central pore-like oral opening surrounded by six inner labial sensilla, fused with submedial lip sectors to produce a distinct dumbbell-shaped *en face* view. Stylet 13.9-15.2 μm long, with small, rounded knobs. Tail 47-54 μm long, conoid with a rounded tip; hyaline terminus not clearly defined.

Males

Body large, 697-1554 μm long, tapering anteriorly; cuticle annulated with large annuli. Head continuous with body, rounded, without annulations. Labial disc fused with submedial lip sectors, forming an elongate head cap. Stylet robust, 13.9-15.2 μm long, round to oval, with a larger cone than the shaft that widens near the junction with the shaft. Shaft cylindrical, widening slightly near junction with knobs. Knobs small, rounded to heart shaped. Lateral field starting posterior to the stylet knobs or slightly behind the head region as two incisures near the metacorpus; areolated lateral field with four incisures. Tail short (4.3-10.5 μm). Spicules 20.8-35.6 μm long, slightly curved ventrally (Fig. 2K-O), with a cylindrical head shape and distinct offset (Fig. 2P-R).

Females

Body pearly white; neck prominent with clear annulation. Perineal pattern oval to squarish; dorsal arch low and rounded to moderately high. Dorsal striae smooth to wavy, with lateral lines weakly demarcated. Phasmids distinct; perivulval region not striated.

Molecular characterisation

The D2-D3 region of the 28S rDNA sequences (PQ454 017, PQ622663, PQ622664, PQ622665; 727 bp; without differences) were closely related to *M. luci* 'SI-Smartno' from Slovenia (LN713300, LN626950, LN626951, LN62 6948) and Brazil (KX130769, KX130766, MK305905), with 0-1 bp differences and 100% similarity. However,

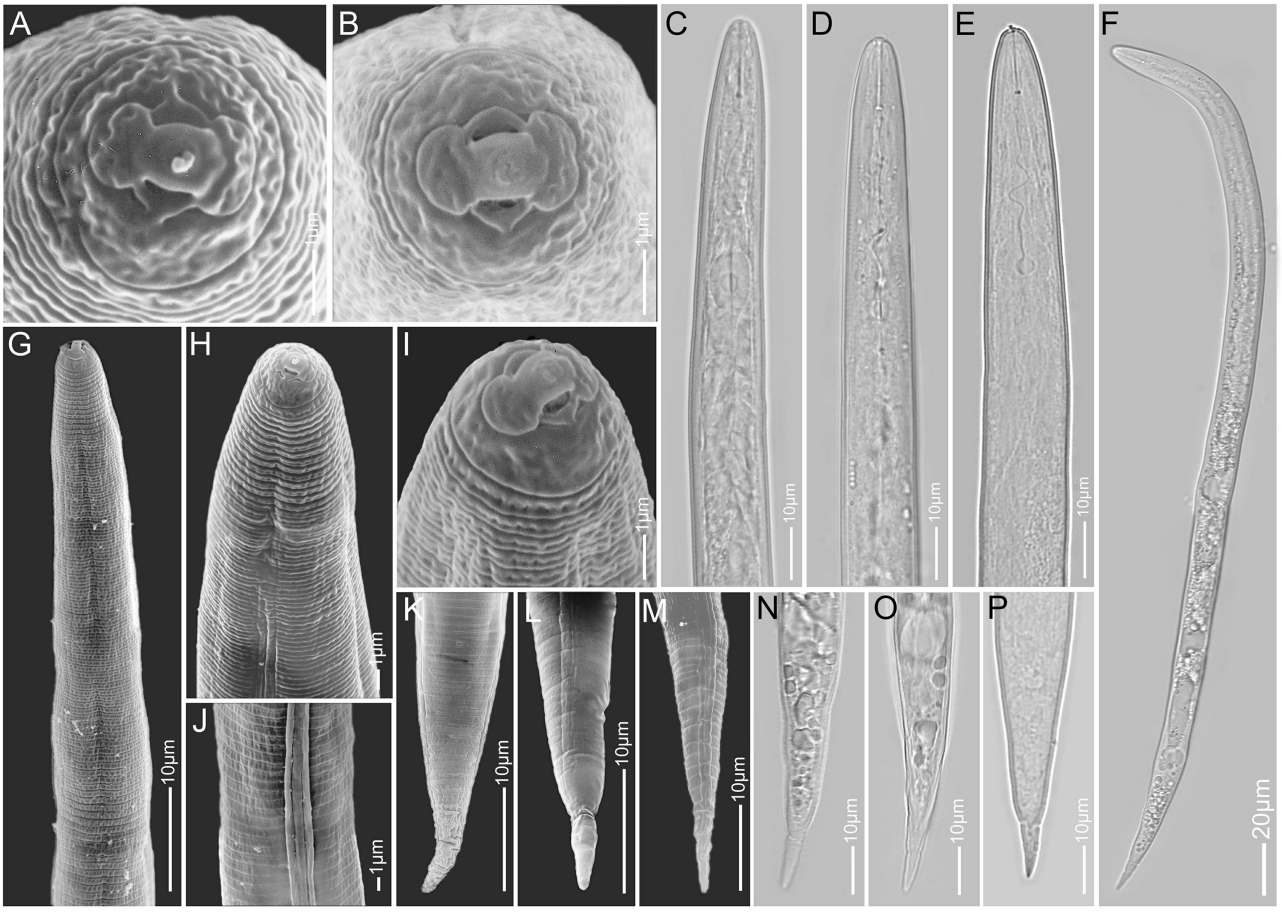

Fig. 1. Scanning electron and light microscopy images of *Meloidogyne luci* second-stage juveniles (J2). A, B: *En face* views; C-E: Anterior body showing stylet, knobs and pharyngeal region; F: Whole body; G-I: Anterior body showing lip region, head lateral view and pharyngeal view; J: Lateral field; K-P: Posterior body showing tail and hyaline part of tail.

phylogenetic analysis placed these sequences in an unresolved clade containing *M. luci*, *Meloidogyne* sp., and *M. hispanica* (0.73 PP) (Fig. 3A). Four ITS rDNA sequences (PQ610424, PQ610425, PQ610426, PQ610427; 540-687 bp; 0-9 bp differences; 98% similarity) showed 97% similarity with 0-21 bp differences of *M. luci* 'SI-Smartno' from Slovenia (LN626963, LN626964, LN626965) and Portugal (KY554194, KY554195, KY554196). Phylogenetic analysis again placed them in an unresolved position with *M. ethiopica*, *M. hispanica*, *M. luci* and *M. enterolobii*, within a maximally supported clade sister to *M. inornata* (Fig. 3B). The two *cox1* mtDNA sequences (PQ448335, PQ610476; 411 bp) were identical to each other and to *M. luci* sequences from GenBank (KU372171, KU372172, MF280974, MF280975, and MF280976; data not shown). Two identical *Nad5* mtDNA sequences (PQ462657, PQ619865; 450 bp) were also identical to *M. luci* sequences available in GenBank (KU372417, KU372418, KU372419), as well as sequences of *M. arenaria* (MT135545, OM418721, MH399824, KU372357) *M. ethiopica* (KU372360), *M. hispanica* (MZ332520, MZ332521, OM418722, OM418729), *M. inornata* (KU372389, KU372390) and *Meloidogyne* sp.1 (KU372421). In phylogenetic trees, these sequences were placed in an unresolved position with *M. ethiopica*, *M. inornata*, *M. hispanica*, *M. arenaria* and *Meloidogyne* sp. in a well-supported clade (0.95 PP; Supplementary Fig. 1A). Four identical *cox2* mtDNA sequences (OQ476238, OQ476239, OQ476240, PQ619863) were also identical to published *M. luci* sequences (MZ393435, KU372209, KU372210, and KU372211). Again, *M. luci* grouped with *M. inornata*,

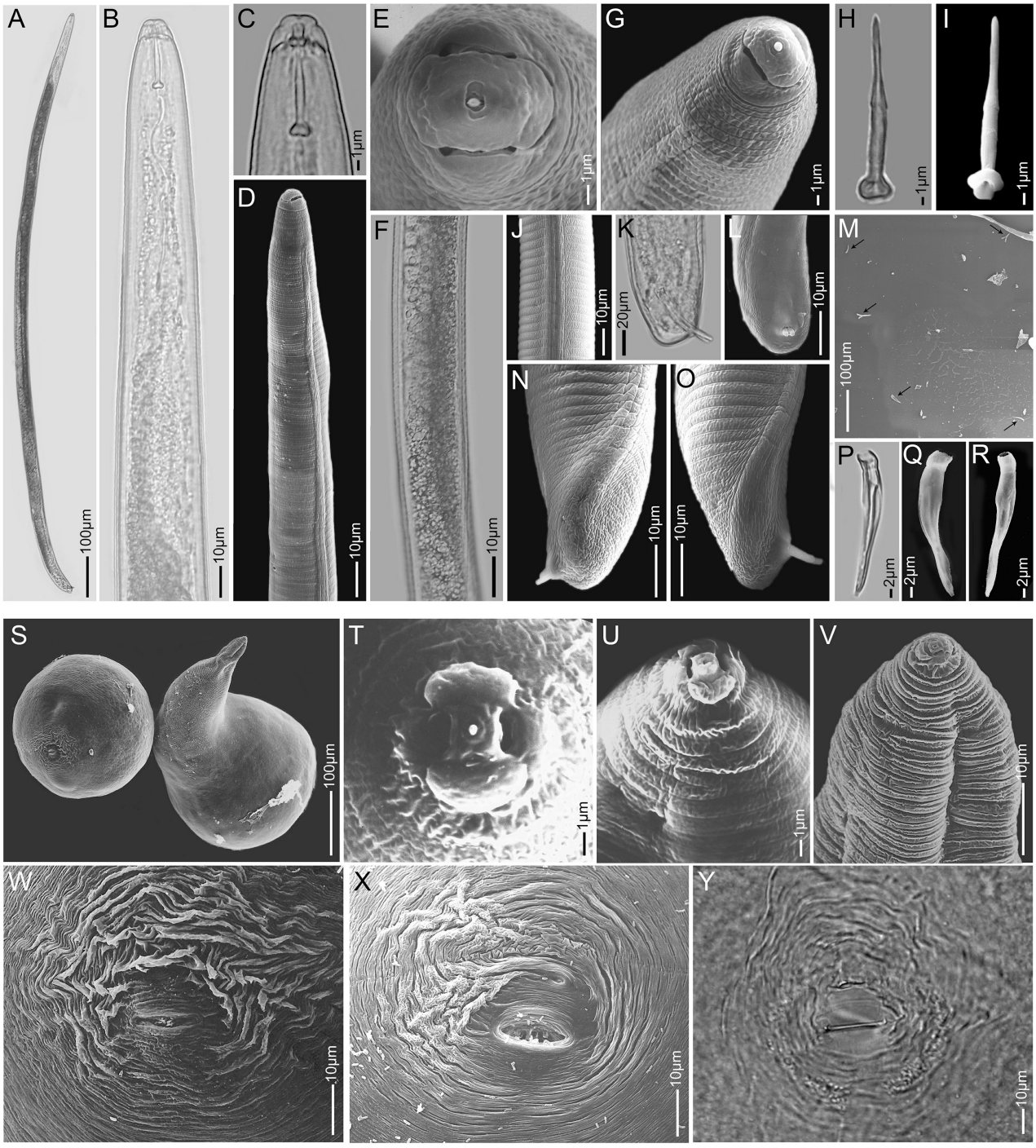

Fig. 2. Light and scanning electron microscopy images of *Meloidogyne luci*. A-R: male; S-Y: Female. A: Whole body of male; B-D, G: Anterior body of males showing lip region and head lateral view; E: *En face* view of male; F: Midbody at level of testes; H, I: Stylet structure; J: Lateral field; K, L, N, O: Posterior body of male showing spicules; M: Visualisation of spicules after excision procedure; P-R: excised spicules; S: Whole body female; T: *En face* of female; U, V: Anterior body of females; W-Y: Female perineal patterns.

Table 2. Morphometric comparison of second-stage juveniles (J2) and males of *Meloidogyne luci* from Ethiopia, and the original description from Brazil, *M. luci* from Slovenia (population SI-Smartno) and Portugal (Carneiro *et al*., 2014; Stare *et al*., 2017; Rusinque *et al*., 2021), *M. ethiopica* from Brazil (Carneiro *et al*., 2004), *M. inornata* from Brazil (Carneiro *et al*., 2008) and *M. hispanica* from Spain (Hirschmann, 1986). All measurements are in μm and in the format mean + standard deviation (range).

Character	*M. luci* from Ethiopia (this study)	*M. luci*, Brazil (Carneiro *et al*., 2014)	*M. luci* 'SI-Smartno', Slovenia (Gerič Stare *et al*., 2019)	*M. luci*, Portugal (Rusinque *et al*., 2021)	*M. ethiopica*, Brazil (Carneiro *et al*., 2004)	*M. inornata*, Brazil (Carneiro *et al*., 2008)	*M. hispanica*, Spain Hirschmann (1986)
Second-stage juveniles (J2)							
n	10	30	20	10	30	30	50
Body length	404 ± 29 (380-438)	383 ± 85 (300-470)	351 ± 29 (321.2-408.0)	405 ± 23 (376-446)	468 ± 3 (326-510)	418 ± 3 (394-487)	393 ± 18.7 (356-441)
Stylet length	14.6 ± 0.5 (13.9-15.2)	12.5 ± 0.2 (12.0-13.5)	13.6 ± 0.4 (13-14)	14.1 ± 1 (11.4-15.6)	12.2 ± 0.1 (11-14)	11.5 ± 0.1 (10-13)	11.1 ± 0.3 (10.4-11.9)
Excretory pore to anterior end	77 ± 11.1 (62-88)	73 ± 10 (62-82)	76.2 ± 10.7 (63-92)	–	93 ± 0.9 (71-106)	158 ± 0.9 (152-164)	80 ± 2.7 (73.9-86)
Tail length	51 ± 2.4 (47-54)	44 ± 4.5 (40-49)	46 ± 5.0 (37.6-58)	47 ± 6 (40-54)	62 ± 0.6 (52-72)	49 ± 0.6 (35.0-58.0)	46 ± 2.8 (41.1-53.4)
Hyaline terminus	13 ± 0.5 (12.5-13.8)	11.7 ± 3.0 (9-15)	11.1 ± 1.4 (8.9-14.0)	11.2 ± 1.97 (9.0-14.1)	13.5 ± 0.2 (12.0-15.0)	13.9 ± 0.25 (10.0-15.0)	11.1 ± 1.6 (9.5-13.7)
Max. body width	18 ± 1.2 (17-20)	16 ± 1.5 (13-20)	15.3 ± 2.1 (12-21.0)	15.9 ± 2.26 (14.6-21)	20 ± 0.3 (15-22)	19.3 ± 0.6 (17.0-22.0)	27.1 ± 1.2 (24.6-30.9)
Males (n = 30)							
Body length	859 ± 240 (697-1554)	1602 ± 520 (1090-2130)	1534 ± 172 (1341-1940)	–	1171 ± 48 (890-1500)	1594 ± 58 (1101-2063)	1668 ± 168 (1341-1990)
Maximum body width	25.5 ± 7.0 (20-34)	43 ± 5.0 (37-50)	37.3 ± 7.2 (29-56)	–	48 ± 0.8 (32-59)	47 ± 0.9 (32-51)	41.2 ± 6.1 (31.4-61.4)
Stylet length	20.4 ± 2.2 (18-23)	22.1 ± 2.7 (21-23.0)	21.2 ± 1.7 (18-24)	–	24.8 ± 0.6 (23-27)	21.7 ± 0.6 (20-25)	23.5 ± 0.6 (21.7-24.3)
Stylet knob heigh	1.7 ± 0.3 (1.3-2.4)	2.6 ± 0.3 (2.5-3.0)	2.8 ± 0.6 (2.0-3.7)	–	3.3 ± 0.1 (3.0-4.0)	3.0 ± 0.5 (2.5-3.5)	3.1 ± 0.2 (2.9-3.5)
Stylet knob width	2.5 ± 0.7 (2-5)	4.2 ± 0.4 (3.8-4.5)	4.2 ± 0.4 (3.3-4.6)	–	4.3 ± 0.6 (3.5-5.0)	4.8 ± 0.6 (4.0-5.0)	5.6 ± 0.3 (5.1-6.1)
DGO	2.9 ± 0.4 (2.2-3)	3.5 ± 1.0 (2.5-4.5)	3.2 ± 0.5 (2.4-3.8)	–	2.5 ± 0.1 (2.0-3.5)	4.5 ± 0.2 (4.0-5.0)	2.5 ± 0.5 (1.4-3.6)
Anterior end to excretory pore	141.8 ± 9.3 (125-152)	199 ± 30.2 (150-217)	150.3 ± 30.2 (111-181)	–	200 ± 31 (187-215)	167.3 ± 3.1 (135-200)	181.5 ± 20.3 (148.6-254.1)
Tail length	5.8 ± 1.8 (4-11)	9.5 ± 1.0 (3.0-15.0)	13.0 ± 2.1 (9.7-18.0)	–	13.4 ± 0.5 (10.2-17.0)	13.5 ± 0.5 (10-15)	13.3 ± 1.7 (10.7-16.2)
Spicule length	25.9 ± 2.8 (21-36)	31.3 ± 4.0 (24.0-35.0)	31.2 ± 3.0 (27.0-37.6)	–	39 ± 0.6 (34-42)	33.0 ± 0.6 (26-38)	32 ± 0.8 (31.1-33.7)

M. hispanica and *M. ethiopica* in a moderately supported clade (0.90 PP; Supplementary Fig. 1B).

Mitochondrial genome of *M. luci*

The complete mitochondrial genome of the Ethiopian *M. luci* isolate was 18 702 bp long, with a base composition of 33.6% A, 5.0% C, 11.4% G, and 49.9% T. Gene prediction by MITOS2 identified 11 open reading frames (ORFs), 8 transfer RNAs (tRNAs; *e*-value < 0.01), and 2 ribosomal RNAs (rRNAs; *e*-value < 0.01) (Fig. 4). BLAST analysis revealed that the Ethiopian isolate showed 99.91% sequence identity with the reference *M. luci* mitochondrial genome 'SI-Smartno V13' (acces-

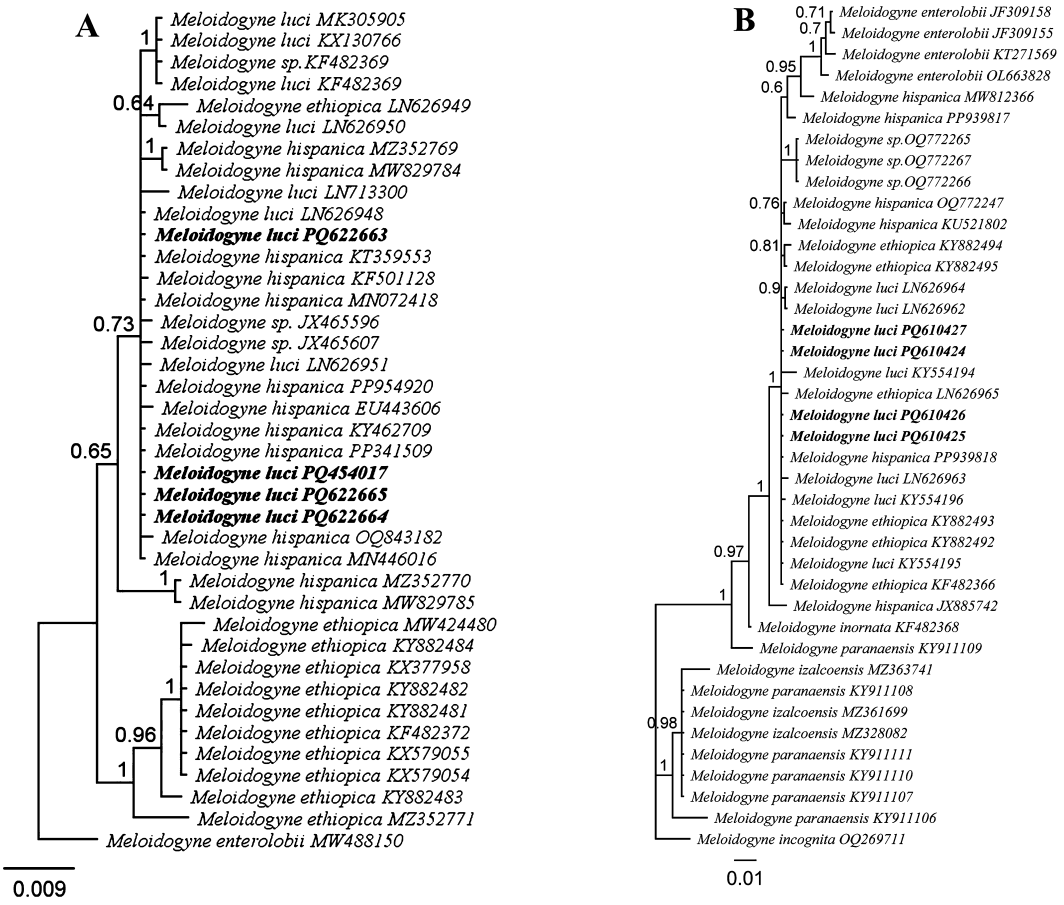

Fig. 3. Bayesian 50% majority rule consensus phylogeny of *Meloidogyne luci* from Ethiopia and related species based on 28S (A) and ITS (B) of rDNA genes using a GTR model. Posterior probability was given next to each node. Sequences of *M. luci* from this study are in bold.

sion CACSLI010000066, project PRJEB27977) from Slovenia. The long-amplicon sequencing strategy enabled full coverage of repetitive regions. The final consensus sequence retained the most frequent tandem repeats identified by CD-HIT within the Decona pipeline. Comparative analysis (Fig. 5) revealed that, relative to the reference genome (Mluci_Seq1_Ref) (Susič *et al*., 2020b), the Ethiopian isolate contained an additional repeat region, one extra open reading frame (ORF) encoding ATP6, and an additional transfer RNA (tRNA), specifically *trnM*. Two tandemly organised repetitive blocks were identified between positions 12 632-14 773 and 15 896-16 210, consisting of 21 and 5 repeat units of 102 bp and 63 bp, respectively.

Phylogenetic analysis and intra *vs* interspecific variability

Phylogenetic RAxML analyses based on complete mitochondrial genomes of *Meloidogyne* species (both trimmed and untrimmed alignments) confirmed the correct taxonomic placement of the Ethiopian *M. luci* isolate within the species (Fig. 6). Sequence similarity among *M. luci* populations was high; the Ethiopian mtDNA shared 99.9% identity with *M. luci* strain 'SI-Smartno V13' from Slovenia, and both formed a highly supported clade (0.99). *Meloidogyne luci* showed 97.9 % similarity with *M. ethiopica* and *M. inornata*, which together formed a maximally supported sister clade (Fig. 6). Despite the high sequence similarity among *Meloidogyne* mitogenomes, the Ethiopian and Slovenian *M. luci* popu-

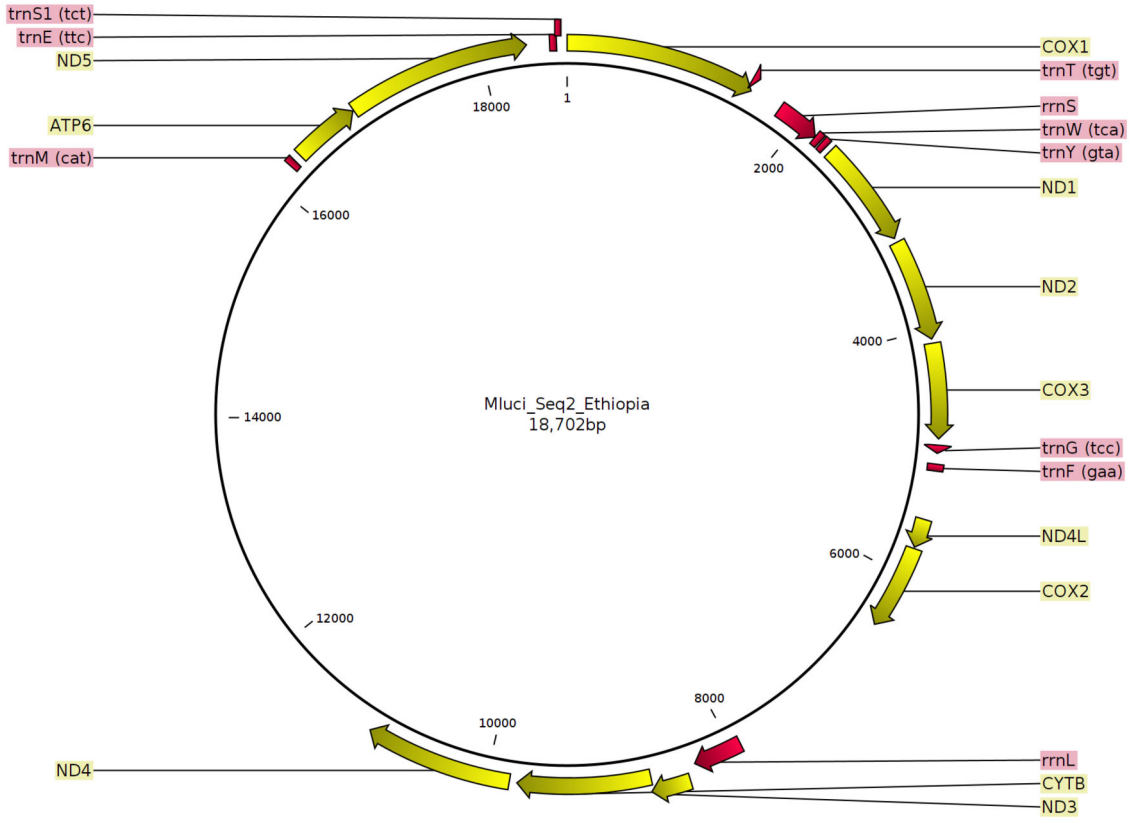

Fig. 4. Complete mitogenome of a *Meloidogyne luci* isolate from Ethiopia. The gene, rRNA and tRNA predictions were made by MITOS2.

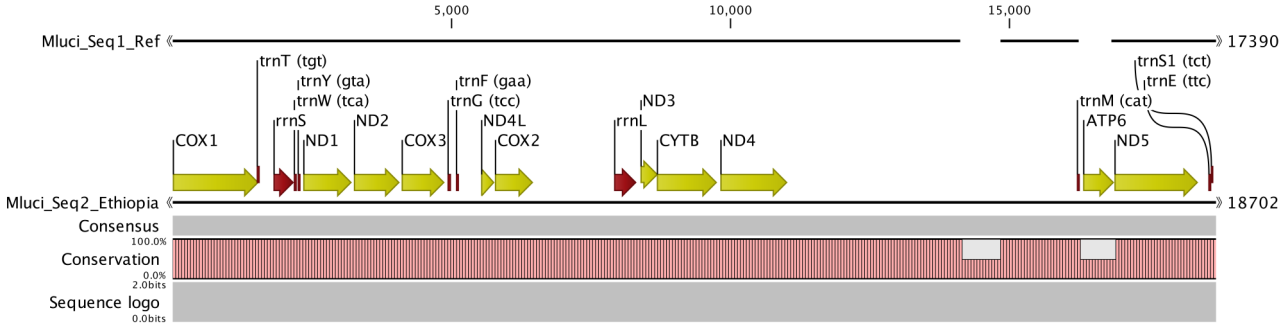

Fig. 5. Alignment between the Ethiopian *Meloidogyne luci* mtDNA and the reference sequence obtained from publicly available data (NCBI WGS database and SRA). The gaps indicate missing parts in the reference mtDNA compared to the Ethiopian sequence.

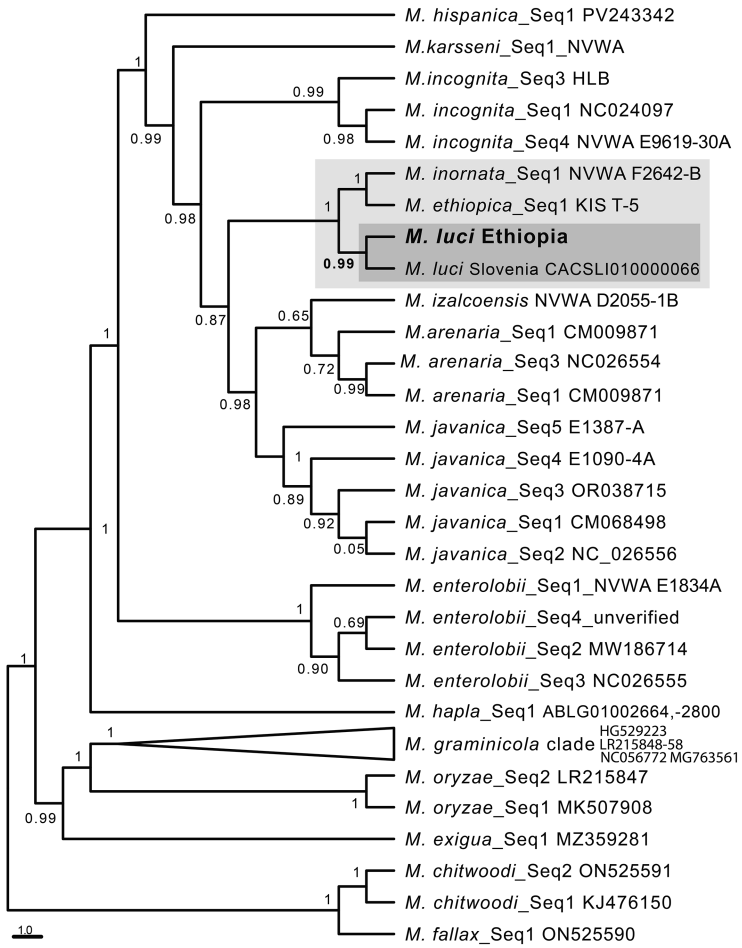

Fig. 6. Phylogenetic RAxML analyses of *Meloidogyne luci* from Ethiopia, based on fully untrimmed mtDNA multiple sequence alignment, generated using ClustalOmega, with comparable *Meloidogyne* mitogenomes. The MSA was highlighted in light grey is the clade containing *M. luci*, *M. ethiopica* and *M. inornata*.

lations are clearly separated from *M. inornata* and *M. ethiopica*.

Host status and plant growth assessment

Following previous pathogenicity results (Kefelegn *et al*., 2025), eight weeks after nematode inoculation, chickpea plants exhibited extensive gall formation (Fig. 7). A clear reduction in plant growth and root biomass was observed, which correlated with increasing nematode density (Table 3).

Discussion

This study provides a comprehensive morphological characterisation of J2, males, and females of *M. luci*, unequivocally linking these features with molecular data from multiple loci and the complete mitogenome. The morphology and morphometrics of the Ethiopian *M. luci* populations are consistent with the original description by Carneiro *et al*. (2014) and subsequent characterisations (Maleita *et al*., 2018; Gerič Stare *et al*., 2019; Rusinque *et al*., 2021). Using SEM, Carneiro *et al.* (2014) demonstrated that stylet knob morphology could be used to distinguish *M. luci* from *M. ethiopica* and *M. inornata*. In the present study, *M. luci* exhibited small, rounded to heart-shaped knobs, consistent with Carneiro *et al.*

Fig. 7. Roots of chickpea 'Arerti' infected with *Meloidogyne luci*, showing extensive galls.

(2014) and clearly distinct from the reniform knobs of *M. ethiopica* and the indented, sloped knobs of *M. inornata* (Carneiro *et al*., 2004, 2008). In both Carneiro *et al*. (2014) and the current study, the morphological characteristics of isolating spicules and stylets were examined using both LM and SEM. Because these structures are minute, isolation and observation under LM typically requires a trained nematologist. Compared with Eisenback's (1985) method, which involves laborious manual handling that can usually only be performed by specialists and carries a higher risk of structural distortion due to acid treatment and drying, our improved centrifugation-based technique offers notable advantages for spicule isolation and is accessible to non-specialists. Moreover, centrifugation minimises the risk of mechanical damage, while repeated washing effectively removes residual chemicals, making this technique optimal for examination under LM and SEM.

In its original species description, the D2-D3 of 28S and ITS regions of rDNA were proposed as useful markers for differentiating *M. luci* from other closely related RKN, as they form distinct clusters (Carneiro *et al*., 2014). Our analyses show that the Ethiopian populations, along with *M. luci* 'SI-Smartno' from Slovenia and those from Brazil, clustered with *M. ethiopica*, *M. hispanica* and an unidentified *Meloidogyne* sp. in the phylogenetic analysis based on the D2-D3 region of 28S rDNA. Similarly, phylogenetic analysis of the ITS rDNA region clustered *M. luci* with *M. ethiopica*, *M. hispanica*, and other unidentified species. This agrees with previous studies by Blok *et al*. (1997), Maleita *et al*. (2018) and Gerič Stare *et al*. (2017), who also reported weak resolution of these markers for differentiating *M. luci* from closely related species. Although most tropical root-knot nematodes can be reliably identified with *Nad5* mtDNA sequences (Janssen *et al*., 2016), the *Nad5* sequences of *M. luci* were found 100% identical to those of *M. arenaria*, *M. ethiopica*, *M. inornata*, *M. hispanica* and *Meloidogyne* sp. Sequencing of the *cox2* region revealed two bp differences from *M. hispanica* and one bp difference from *M. ethiopica*, but 100% identical to *M. inornata* and *M. arenaria*. The *cox1* mtDNA region did not resolve *M. luci* from *M. arenaria*, *M. ethiopica*, *M. inornata*, or *M. hispanica*, in contrast to Maleita *et al*. (2018), who found *cox1* to be informative to differentiate *M. luci* from *M. ethiopica*. Taken together, even after analysing multiple loci, distinguishing *M. luci* from *M. hispanica* remains impossible. In Kefelegn *et al*. (2025), a robust identification of *M. luci* was achieved only by combining species-specific PCR amplification with esterase isozyme (EST) profiling, highlighting the critical role of EST analyses in differentiating tropical root-knot nematodes.

In the present study, full mitogenome sequencing provided clear separation of *M. luci* from *M. hispanica* and its closest relatives, confirming its diagnostic power. The mitogenome presented here constitutes the first complete *M. luci* mitogenome characterised from Africa. The presence of additional repeat regions and extra coding elements, such as *atp6* and *trnM*, may reflect intraspecific variation within *M. luci*. The presence of *atp6* and *trnM* in our *M. luci* mitogenome does not imply that these genes are unique to this species, as *atp6* is expected to occur in all *Meloidogyne* mitogenomes (Janssen *et al*., 2016). Rather, our results demonstrate that long-amplicon Nanopore sequencing enabled recovery of genomic regions that were missing from previously published *M. luci* assemblies generated from short-read Illumina (Susič *et al*., 2020b). The ability to obtain high-quality mitogenomes underscores the effectiveness of long-amplicon Nanopore sequencing for resolving complex and repetitive regions in eukaryotic mitochondrial DNA (Kinkar *et al*., 2021; Furuta *et al*., 2025). Impor-

Table 3. The host-status of chickpea 'Arerti' cultivar inoculated at different initial population densities (P_i) of *Meloidogyne luci*. where: P_f, final population; RF, reproduction factor (P_f/P_i), plant height, and fresh root weight (FRW) with standard deviation (SD) eight weeks after inoculation.

P_i (J2 pot^{-1})	P_f (J2 pot^{-1})	RF (= P_f/P_i)	Plant height (cm)	SD plant height	FRW (g)	SD FRW
1000	31 000	31	59	±14.9	13	±5.0
4000	46 000	11.5	41	±3.1	9.4	±1.7
8000	76 000	9.5	33	±3.51	5.6	±0.98

tantly, full mitogenome sequencing offers a substantial improvement over traditional barcoding for nematode diagnostics (Kern *et al*., 2020; Jain *et al*., 2025). It is well established that complete mitochondrial and nuclear genomes provide much higher taxonomic resolution than single-marker approaches (Abad *et al*., 2008; Lunt *et al*., 2014; Burke *et al*., 2015; Phan *et al*., 2020; Singh *et al*., 2022). Mitogenome data enable high-resolution phylogenetic analyses that clarify relationships often unresolved by nuclear markers such as SSU rDNA or by individual mitochondrial genes (Kern *et al*., 2020; Gendron *et al*., 2023). Furthermore, mitogenome sequencing is cost-effective and computationally manageable, offering robust taxonomic identification and new insights into nematode diversity (Jain *et al*., 2025). Collectively, these results demonstrate that integrating complete mitogenome sequencing with long-read barcoding, combining mitochondrial and ribosomal sequences, can substantially improve species-level diagnostics (Singh *et al*., 2022; Noshadi *et al*., 2026). As sequencing costs continue to fall, such integrative genomic approaches are expected to become standard in nematode diagnostic workflows (Pun *et al*., 2024; Ogbuji & Agogbua, 2025).

In summary, this study provides the first comprehensive morphological and genomic characterisation of *M. luci* from Africa. Traditional single-gene barcoding markers based on rDNA or mtDNA did not resolve *M. luci* from closely related species. However, complete mitogenome sequencing clearly differentiated *M. luci* and revealed intraspecific variation, underscoring its diagnostic value. The improved centrifugation-based technique described here also enhances the morphological study of male spicules. Together, these advances strengthen the taxonomy and molecular diagnostics of tropical root-knot nematodes and highlight the importance of complete mitogenome data for resolving closely related *Meloidogyne* species. Given the multiplication of *M. luci* on the tested chickpea cultivar, and its polyphagous nature, further studies in Ethiopia should assess its distribution, prevalence, and host status on other major crops. Such information will be critical for designing an integrated nematode management approach aimed at preventing economically damaging population densities on farmers' fields.

Acknowledgements

This work was supported by Ghent University Special Research Fund (UGent 01W04120), Flanders Research Institute for Agriculture, Fisheries and Food (ILVO, Belgium), Jimma and Debre Berhan Universities, Ethiopia, Slovenian Research and Innovation Agency (ARIS grants P4-0072, P4-0431), and HORIZONEUROPE Food, Bioeconomy, Natural Resources, Agriculture and Environment (grant 101083727; NEM-EMERGE). The authors gratefully acknowledge Anne-Marie Deeren for her invaluable assistance in culturing all root-knot nematode populations.

References

Abad, P., Gouzy, J., Aury, J.M., Castagnone-Sereno, P., Danchin, E.G., Perfus-Barbeoch, L., Anthouard, V., Artiguenave, F., Blok, V.C. *et al.* (2008). Genome sequence of the metazoan plant-parasitic nematode. *Meloidogyne incognita. Nature Biotechnology* 26, 909-915. DOI: 10.1038/nbt.1482

Bačić, J., Pavlović, M., Kušić-Tišma, J., Širca, S., Theuerschuh, M. & Gerič Stare, B. (2023). First report of the root-knot nematode *Meloidogyne luci* on tomato in Serbia. *Plant Disease* 107, 2554. DOI: 10.1094/PDIS-01-23-0164-PDN

Bellé, C., Balardin, R., Ramos, R.F., Sobucki, L., Gabriel, M. & Antoniolli, Z.I. (2016). First report of *Meloidogyne luci* parasitizing *Glycine max* in Brazil. *Plant Disease* 100, 2174. DOI: 10.1094/PDIS-05-16-0624-PDN

Blok, V.C., Phillips, M.S. & Fargette, M. (1997). Comparison of sequences from the ribosomal DNA intergenic region of *Meloidogyne mayaguensis* and other major tropical root-knot nematodes. *Journal of Nematology* 29, 16-22.

Bowles, J., Blair, D. & McManus, D.P. (1992). Genetic variants within the genus *Echinococcus* identified by mitochondrial-

DNA sequencing. *Molecular and Biochemistry Parasitology* 54, 165-174. DOI: 10.1016/0166-6851(92)90109-w

Burke, M., Scholl, E.H., Bird, D.M., Schaff, J.E., Colman, S.D., Crowell, R., Diener, S., Gordon, O., Graham, S., Wang, X., Windham, E., Wright, G.M. & Opperman, C.H. (2015). The plant parasite *Pratylenchus coffeae* carries a minimal nematode genome. *Nematology* 17, 621-637. DOI: 10.1163/15685411-00002901

Carneiro, R.M.D.G., Gomes, C.B., Almeida, M.R.A., Gomes, A.C.M.M. & Martins, I. (2003). First record of *Meloidogyne ethiopica* Whitehead, 1968 on kiwi in Brazil and reaction on different plant species. *Nematologia Brasileira* 27, 151-158.

Carneiro, R.M.D.G., Randing, O., Almeida, M.R.A. & Gomes, A.C. (2004). Additional information on *Meloidogyne ethiopica* Whitehead, 1968 (Thylenchida: Meloidogynidae) a root-knot nematode parasitizing kiwi fruit and grapevine from Brazil and Chile. *Nematology* 6, 109-123. DOI: 10.1163/156854104323072982

Carneiro, R.M.D.G., Mendes, M.L., Almeida, M.R.A., Santos, M.F.A., Gomes, A.C. & Karssen, G. (2008). Additional information on *Meloidogyne inornata* Lordello, 1956 (Tylenchida: Meloidogynidae) and its characterization as a valid species. *Nematology* 10, 123-136.

Carneiro, R.M.D.G., Correa, V.R., Almeida, M.R.A., Gomes, A.C.M.M., Deimi, A.M., Castagnone-Sereno, P. & Karssen, G. (2014). *Meloidogyne luci* n. sp. (Nematoda: Meloidogynidae), a root-knot nematode parasitising different crops in Brazil, Chile and Iran. *Nematology* 16, 289-301. DOI: 10.1163/15685411-00002765

Conceição, I.L., Tzortzakakis, E.A., Gomes, P., Abrantes, I. & da Cunha, M.J. (2012). Detection of the root-knot nematode *Meloidogyne ethiopica* in Greece. *European Journal of Plant Pathology* 134, 451-457. DOI: 10.1007/s10658-012-0027-0

De Ley, P., Félix, M.A., Frisse, L.M., Nadler, S.A., Sternberg, P.W. & Thomas, W.K. (1999). Molecular and morphological characterization of two reproductively isolated species with mirror-image anatomy (Nematoda: Cephalobidae). *Nematology* 1, 591-612.

Derycke, S., Vanaverbeke, J., Rigaux, A., Backeljau, T. & Moens, T. (2010). Exploring the use of cytochrome oxidase *c* subunit 1 (*COI*) for DNA barcoding of free-living marine nematodes. *Plos One* 5(10), e13716. DOI: 10.1371/journal.pone.0013716

Donath, A., Jühling, F., Al-Arab, M., Bernhart, S.H., Reinhardt, F., Stadler, P.F., Middendorf, M. & Bernt, M. (2019). Improved annotation of protein-coding genes boundaries in metazoan mitochondrial genomes. *Nucleic Acids Research* 47, 10543-10552. DOI: 10.1093/nar/gkz833

Doorenspleet, K., Jansen, L., Oosterbroek, S., Kamermans, P., Bos, O., Wurz, E., Murk, A. & Nijland, R. (2025). The long and the short of it: nanopore based eDNA metabarcoding of marine vertebrates works; sensitivity and specificity depend on amplicon lengths. *Molecular Ecology Resource* 25, e14079. DOI: 10.1111/1755-0998.14079

Eisenback, J.D. (1985). Detailed morphology and anatomy of second-stage juveniles, males, and females of the genus *Meloidogyne* (root-knot nematodes). In: Sasser, J.N. & Carter, C. (Eds). *An advanced treatise on* Meloidogyne*, vol. 1. Biology and control*. Raleigh, NC, USA, North Carolina State University Graphics, pp. 47-77.

EPPO (2023). A2 and A1 list of pests recommended for regulation as quarantine pests. Avalable at https://www.eppo.int/ACTIVITIES/plant_quarantine/A2_list

FAOSTAT (2022). FAOSTAT. Available at http://www.fao.org/faostat/en/data/QC/visualize

Furuta, Y., Kakita, M. & Tanaka, H. (2025). MitoCOMON: whole mitochondrial DNA sequencing by primer design and long overlapping amplicon assembly. *BMC Genomics* 26, 787. DOI: 10.1186/s12864-025-12010-0

Gendron, E.M., Sevigny, J.L., Byiringiro, I., Thomas, W.K., Powers, T.O. & Porazinska, D.L. (2023). Nematode mitochondrial metagenomics: A new tool for biodiversity analysis. *Molecular Ecology Resources* 23, 1598-1613. DOI: 10.1111/1755-0998.13761

Gerič Stare, B., Strajnar, P., Susič, N., Urek, G. & Širca, S. (2017). Reported populations of *Meloidogyne ethiopica* in Europe identified as *Meloidogyne luci*. *Plant Disease* 101, 1627-1632. DOI: 10.1094/PDIS-02-17-0220-RE

Gerič Stare, B., Aydinli, G., Devran, Z., Mennan, S., Strajnar, P., Urek, G. & Širca, S. (2019). Recognition of species belonging to *Meloidogyne ethiopica* group and development of a diagnostic method for its detection. *European Journal of Plant Pathology* 154, 621-633. DOI: 10.1007/s10658-019-01686-2

Hirschmann, H. (1986). *Meloidogyne hispanica* n. sp. (Nematoda: Meloidogynidae), the 'Seville Root-Knot Nematode'. *Journal of Nematology* 18, 520-532.

Jain, A., Li, T., Wainer, J., Edwards, J., Rodoni, B.C. & Sawbridge, T.I. (2025). High-throughput sequencing enables rapid analyses of nematode mitochondrial genomes from an environmental sample. *Pathogens* 14, 234. DOI: 10.3390/pathogens14030234

Janssen, T., Karssen, G., Verhaeven, M., Coyne, D. & Bert, W. (2016). Mitochondrial coding genome analysis of tropical root-knot nematodes (*Meloidogyne*) supports haplotype-based diagnostics and reveals evidence of recent reticulate evolution. *Scientific Reports* 6, 2259. DOI: 10.1038/srep22591

Jones, J.T., Haegeman, A., Danchin, E.G., Gaur, H.S., Helder, J., Jones, M.G.K., Kikuchi, T., Manzanilla-López, R., Palomares-Rius, J.E., Wesemael, W.M. *et al.* (2013). Top 10 plant-parasitic nematodes in molecular plant pathology. *Molecular Plant Pathology* 14, 946-961. DOI: 10.1111/mpp.12057

Kefelegn, H., Meressa, B.H., Yon, S., Couvreur, M., Wesemael, W.M.L., Teklu, M.G. & Bert, W. (2023). First reports and morphological and molecular characterization of *Pratylenchus delattrei* and *Quinisulcius capitatus* associated with

chickpea in Ethiopia. *Journal of Nematology* 55, 1-13. DOI: 10.2478/jofnem-2023-0027

Kefelegn, H., Meressa, B.H., Yon, S., Couvreur, M., Wesemael, W.M.L., Teklu, M.G. & Bert, W. (2024). Diversity of plant parasitic nematodes associated with chickpea (*Cicer arietinum* L.) in the main growing areas of Ethiopia. *Nematology* 26, 491-518. DOI: 10.1163/15685411-bja10318

Kefelegn, H., Couvreur, M., Meressa, B.H., Wesemael, W.M.L., Teklu, M.G. & Bert, W. (2025). First Report of root-knot nematode, *Meloidogyne luci*, parasitizing chickpea (*Cicer arietinum*) in Ethiopia. *Plant Disease* 109, 1384. DOI: 10.1094/PDIS-01-25-0096-PDN

Kern, E.M.A., Kim, T. & Park, J.K. (2020). The mitochondrial genome in nematode phylogenetics. *Fronter in Ecology and evolution* 8, 250. DOI: 10.3389/fevo.2020.00250

Kinkar, L., Gasser, R.B., Webster, B.L., Rollinson, D., Littlewood, D.T.J., Chang, B.C.H., Stroehlein, A.J., Korhonen, P.K. & Young, N.D. (2021). Nanopore sequencing resolves elusive long tandem-repeat regions in mitochondrial genomes. *International Journal of Molecular Science* 22, 1811. DOI: 10.3390/ijms22041811

Lunt, D.H., Kumar, S., Koutsovoulos, G. & Blaxter, M.L. (2014). The complex hybrid origins of the root knot nematodes revealed through comparative genomics. *PeerJ* 2, e356. DOI: 10.7717/peerj.356

Maleita, C., Esteves, I., Cardoso, J.M.S., Cunha, M.J., Carneiro, R.M.D.G. & Abrantes, I. (2018). *Meloidogyne luci*, a new root-knot nematode parasitizing potato in Portugal. *Plant Pathology* 67, 366-376. DOI: 10.1111/ppa.12202

Maleita, C., Cardoso, J.M.S., Rusinque, L., Esteves, I. & Abrantes, I. (2021). Species-specific molecular detection of the root knot nematode *Meloidogyne luci*. *Biology* 14, 775. DOI: 10.3390/biology10080775

Mandefro, W. & Dagne, K. (2000). Cytogenetic and esterase isozyme variation of root-knot nematode populations from Ethiopia. *African Journal of Plant Protection* 10, 39-47.

Meressa, B.H., Heuer, H., Dehne, H.W. & Hallmann, J. (2014). First report of the root-knot nematode *Meloidogyne hapla* parasitizing roses in Ethiopia. *Plant Disease* 98, 1286. DOI: 10.1094/PDIS-04-14-0383-PDN

Mota, M.M. & Eisenback, J.D. (1993). Morphology of second-stage juveniles and males of *Globodera tabacum tabacum*, *G. t. virginiae* and *G. t. solanacearum* (Nematoda: Heteroderinae). *Journal of Nematology* 25, 27-33.

Noshadi, A., Ghaderi, R., Nielsen, U.N., Hayden, H.L. & He, J.Z. (2026). Paving the way for deeper insights into nematode community composition with long read metabarcoding: ecological and biogeographical coverage of the sequences. *Soil Biology and Biochemistry* 212, 110001. DOI: 10.1016/j.soilbio.2025.110001

Ogbuji, N.G. & Agogbua, J.U. (2025). Genomics in plant pathogen identification and control. *Fronter Plant Science* 16, 1661432. DOI: 10.3389/fpls.2025.1661432

Onkendi, E.M., Kariuki, G.M., Marais, M. & Moleleki, L.N. (2014). The threat of root-knot nematodes (*Meloidogyne* spp.) in Africa: a review. *Plant Pathology* 63, 727-737.

Phan, N.T., Orjuela, J., Danchin, E.G.J., Klopp, C., Perfus-Barbeoch, L., Kozlowski, D.K., Koutsovoulos, G.D., Lopez-Roques, C., Bouchez, O., Zahm, M. *et al.* (2020). Genome structure and content of the rice root-knot nematode (*Meloidogyne graminicola*). *Ecology Evolution* 10, 11006-11021. DOI: 10.1002/ece3.6680

Pun, T.B., Thapa Magar, R., Koech, R., Owen, K.J. & Adorada, D.L. (2024). Emerging trends and technologies used for the identification, detection, and characterization of plant-parasitic nematode infestation in crops. *Plants* 13, 3041. DOI: 10.3390/plants13213041

Rice, P., Longden, I. & Bleasby, A. (2000). EMBOSS: the European Molecular Biology Open Software Suite. *Trends Genetentics* 16, 276-277. DOI: 10.1016/s0168-9525(00)02024-2

Rusinque, L., Nóbrega, F., Cordeiro, L., Serra, C. & Inácio, M.L. (2021). First detection of *Meloidogyne luci* (Nematoda: Meloidogynidae) parasitizing potato in the Azores, Portugal. *Plants* 10, 99. DOI: 10.3390/plants10010099

Santos, D., Correia, A., Abrantes, I. & Maleita, C. (2019). New hosts and records in Portugal for the root-knot nematode *Meloidogyne luci*. *Journal of Nematology* 51, 1-4. DOI: 10.21307/jofnem-2019-003

Seid, A., Fininsa, C., Mekete, T.M., Janssen, T., Decraemer, W. & Wesemael, W. (2019). Biodiversity of *Meloidogyne* spp. from major tomato growing areas of Ethiopia. *European Journal of Plant Pathology* 154, 513-528. DOI: 10.1007/s10658-019-01674-6

Şen, F. & Aydinli, G. (2021). Host status of cultivated crops to *Meloidogyne luci*. *European Journal of Plant pathology* 161, 607-618. DOI: 10.1007/s10658-021-02346-0

Sharma, S.B., Smith, D.H. & McDonald, D. (1992). Nematode constraints of chickpea and pigeon pea production in the semi-arid tropics. *Plant Disease* 76, 868-874.

Singh, P.R., Couvreur, M., Decraemer, W. & Bert, W. (2019). Survey of slug-parasitic nematodes in East and West Flanders, Belgium, and description of *Angiostoma gandavensis* n. sp. (Nematoda: Angiostomidae) from arionid slugs. *Journal of Helminthology* 94, 1-11. DOI: 10.1017/S0022149X19000105

Singh, P.R., Karssen, G., Couvreur, M., Subbotin, S.A. & Bert, W. (2021). Integrative taxonomy and molecular phylogeny of the plant-parasitic nematode genus *Paratylenchus* (Nematoda: Paratylenchinae): linking species with molecular barcodes. *Plants* 10, 408. DOI: 10.3390/plants10020408

Singh, P.R., van de Vossenberg, B.T.L.H., Rybarczyk-Mydłowska, K., Kowalewska-Groszkowska, M., Bert, W. & Karssen, G. (2022). An integrated approach for synonymization of *Rotylenchus rhomboides* with *R. goodeyi* (Nematoda: Hoplolaimidae) reveals high intraspecific mitogenomic variation. *Phytopathology* 112, 1152-1164. DOI: 10.1094/PHYTO-08-21-0363-R

Subbotin, S.A., Palomares-Rius, J.E. & Castillo, P. (2021). *Systematics of root-knot nematodes (Nematoda: Meloidogynidae). Nematology Monographs and Perspectives, Volume 14* (Series Editors: Hunt, D.J. & Perry, R.N.). Leiden, The Netherlands, Brill.

Susič, N., Širca, S., Urek, G. & Gerič Stare, B. (2020a). *Senecio vulgaris* L. recorded as a new host plant for the root-knot nematode *Meloidogyne luci*. *Acta agriculturae Slovenica* 115, 495-497. DOI: 10.14720/aas.2020.115.2.1514

Susič, N., Koutsovoulos, G.D., Riccio, C., Danchin, E.G.J., Blaxter, M.L., Lunt, D.H., Strajnar, P., Širca, S., Urek, G. & Gerič Stare, B. (2020b). Genome sequence of the root-knot nematode *Meloidogyne luci*. *Journal of Nematology* 52, 1-5. DOI: 10.21307/jofnem-2020-025

Vrain, T.C., Wakarchuk, D.A., Levesque, A.C. & Hamilton, R.I. (1992). Intraspecific rDNA restriction fragment length polymorphism in the *Xiphinema americanum* group. *Fundamental and Applied Nematology* 15, 563-573.

Whitehead, A.G. (1968). Taxonomy of *Meloidogyne* (Nematoda: Heteroderidae) with description of four new species. *Transactions of the Zoological Society of London* 31, 263-401.

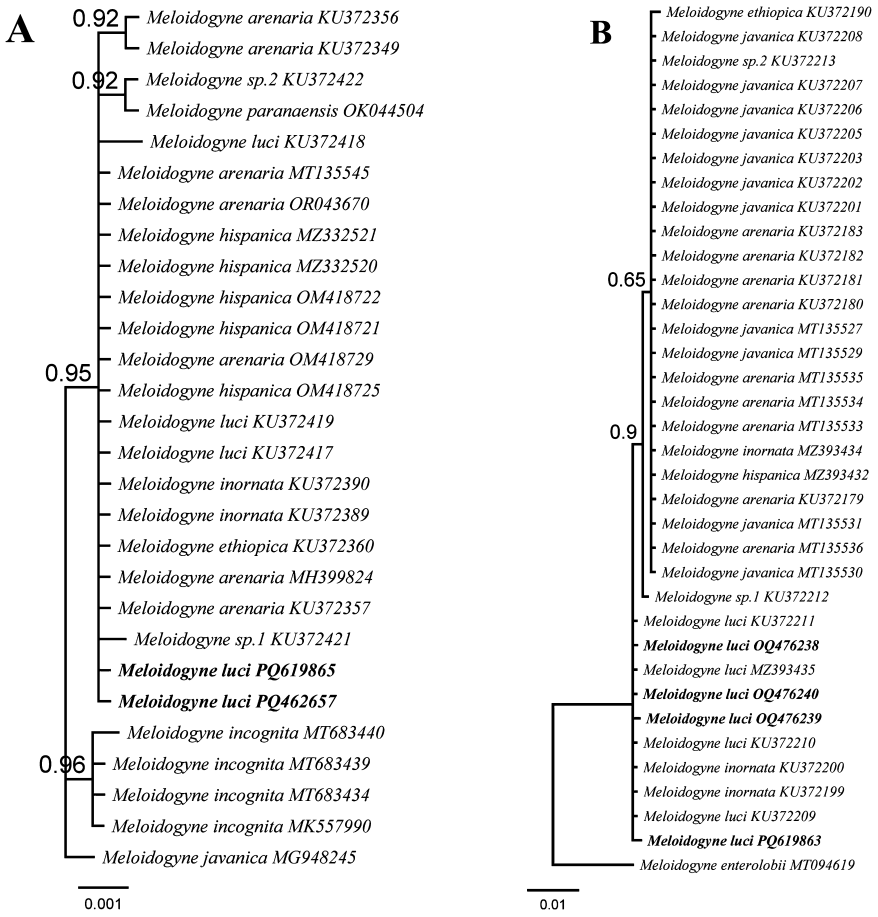

Supplementary Figure S1. Bayesian 50% majority rule consensus phylogeny of *Meloidogyne luci* from Ethiopia and related species based on *Nad5* (A) and *cox2* (B) of mtDNA genes using a GTR model. Posterior probability was given next to each node. Sequences of *M. luci* from this study are in bold.